Scale-free Functional Connectivity Analysis from Source Reconstructed MEG Data

D. La Rocca, P. Ciuciu, V. van Wassenhove
CEA/NeuroSpin, Univ. Saclay, France.
INRIA Parietal, France.
firstname.lastname@cea.fr

H. Wendt
IRIT, Univ. Toulouse, CNRS, Toulouse, France.
herwig.wendt@irit.fr

P. Abry, R. Leonarduzzi
Univ Lyon, Ens de Lyon, Univ Claude Bernard, CNRS, Laboratoire de Physique, Lyon, France.
firstname.lastname@ens-lyon.fr

***Abstract*—Scale-free dynamics, quantified as power law spectra from magnetoencepholagraphic (MEG) recordings of Human brain activity, may play an important role in cognition and behavior. To date, their characterization remain limited to univariate analysis. Independently, functional connectivity analysis usually entails uncovering interactions between remote brain regions. In MEG, specific indices (e.g., Imaginary coherence ICOH and weighted Phase Lag Index wPLI) were developed to quantify phase synchronization between time series reflecting activities of distant brain regions and applied to oscillatory regimes (e.g., α-band in (8, 12) Hz). No such indices has yet been developed for scale-free brain dynamics. Here, we propose to design new indices (w-ICOH and w-wPLI) based on complex wavelet analysis, dedicated to assess functional connectivity in the scale-free regime. Using synthetic multivariate scale-free data, we illustrate the potential and efficiency of these new indices to assess phase coupling in the scale-free dynamics range. From MEG data (36 individuals), we demonstrate that w-wPLI constitutes a highly sensitive index to capture significant and meaningful group-level changes of phase couplings in the scale-free (0.1, 1.5) Hz regime between rest and task conditions.**

I. Introduction

Context: Scale-free brain dynamics. The Human brain is a complex biological system characterized by hierarchical rhythmic activity, which may play an important role in perception and cognition. In the last century, brain activity recorded with electro-, and then, magneto-encephalography (EEG/MEG) has been understood as originating from the synchronous activation of neuronal populations that generate rhythmic activity in predetermined frequency bands. The α-oscillations (8-12 Hz) are spontaneous and most salient during rest, neuroscientists also described additional oscillatory regimes, for instance the β (13-30 Hz) and γ (31-100 Hz) bands readily modulated during task (e.g., decision making, multisensory integration). Recently, broadband *scale-free brain activity* reflecting arrhythmic or irregular dynamics (i.e., without characteristic frequency) has been of increasing interest. Scale-free brain activity is characterized by $1/f$ power law spectra at low frequencies (< 2 Hz), and hypothesized to play a role in brain functions [1]. It is now well established that the accurate modeling and assessment of scale-free dynamics requires replacing spectral estimation with wavelet analysis using self-similarity as a model [2]. The modulation of scale-free dynamics, as quantified by the self-similarity exponent H, was observed when contrasting rest and task-related brain activity, including in different "unconscious" sleep stages [1], [3]–[6].

Related work: functional connectivity assessment. So far, scale-free activity has been characterized in a univariate manner, both in sensor and source space (e.g. [1], [4], [5]). However, remote brain regions are known to interact within large scale functional networks [7] which mediate the information flow inside the brain integrating the activity of functionally segregated modules. These interactions in the brain are referred to as *functional connectivity* (FC) and usually captured by evaluating a similarity index within multivariate neuroimaging data. Classically, such measures are based on cross-correlations or cross-spectra for the oscillatory bands, while the use of the wavelet coherence function was proposed for scale-free dynamics, relying on a concept of fractal connectivity (see, e.g., [8], [9] and references therein). However, redundancies in measurements collected by close-by electrodes limit the effectiveness of these indices for FC assessment in M/EEG because they are highly sensitive to common source effects inducing spurious instantaneous (i.e., delay-free) coupling. For oscillatory regimes, alternative phase synchronization measures, robust to such spurious functional coupling, were proposed and are commonly used in M/EEG to assess FC in given frequency bands, see, e.g., [10], [11]. These indices typically rely on the insensitivity of the imaginary part of the complex normalized cross-spectrum (coherency) to instantaneous coupling (see Section II-A). Yet, for the scale-free dynamics, phase coupling indices for FC assessment in M/EEG are currently lacking.

Goals and contributions. The present work aims to overcome this fundamental limitation and to propose tools for the assessment of FC from scale-free brain dynamics, that are robust to spurious functional coupling and benefit from the theoretical grounding and estimation performance of multiscale analysis for scale-free data. To that end, in Section II-A, we briefly recall the tools classically used in MEG data analysis for brain connectivity assessment in oscillatory bands. The key intuitions underlying these tools constitute also the leading idea for the proposed approach and are translated to scale-free dynamics analysis. To do so, we rely on another key ingredient, the complex wavelet transform. The methodology and corresponding scale-free FC indices are defined in Sec-

ISBN 978-90-827970-1-5

tion II-B and constitute, to the best of our knowledge, the first operational tool for the relevant assessment of FC in the scale-free regime for MEG data. MATLAB codes, implemented by ourselves, will be made available at the time of publication. The proposed approach is illustrated on synthetic scale-free signals and extensively tested on rest and task-related MEG data described in Section III and [12]. Achieved results (Section IV) demonstrate that the proposed tool captures well significant variations of long range phase synchronization in scale-free dynamics between rest and task-related MEG data.

II. Functional connectivity assessment for MEG

A. Oscillatory-based FC analysis in the frequency domain

M/EEG measurements are generally based on non-invasive recordings of simultaneous time-series reflecting whole brain activity. The assessment of statistical relationships within such multivariate data allows for the identification of functional brain networks that are activated in a particular mental state, task execution or health condition. Most FC analyses in M/EEG have exploited complex-valued measures defined in the frequency domain (e.g. the cross-spectrum $S_{mm'}(f)$ of signals Y_m and $Y_{m'}$, or the spectral coherency) given the known oscillatory components of brain dynamics [13], [14]. Yet, the real component of these measures have shown to be strongly affected by volume conduction inducing spurious statistical dependence between recorded time-series [15]. Specifically, the linearity of the Maxwell equations and the quasi-static approximation of the forward model below 100 Hz, allow to assume the linear mixing of sources modeling the volume conduction effect on MEG sensors $Y_m(f)$, and the instantaneous mapping of sources to sensors. The latter assumption implies that the conducted electro-magnetic activity of a single source spatially affects separate sensors with negligible time delay. It follows that the superposition of K *independent* sources $Y_m(f) = \sum_{k=1}^{K} a_{mk} s_k(f)$, recorded at sensors $Y_m(f)$, with coefficients $a_{mk} \in \mathbb{R}$, yields a real-valued cross-spectrum,

$$S_{mm'}(f) = \sum_k a_{mk} a_{m'k} \left| s_k(f) \right|^2 \qquad (1)$$

and so for the coherency, too. It's worth notice that further non-zero imaginary components of $S_{mm'}$ would originate in the presence of dependent sources. In sensor space volume conduction thus strongly affects the real part of the coherency but does not create a non-vanishing imaginary part. The solution of the linear inverse MEG problem should theoretically account for this volume conduction effect to estimate source-reconstructed time series. However, practical solutions to this ill-posed problem entail residual spurious FC in the source space.

Robust phase syncronization measures. Following the above intuition, several robust FC measures, exploiting the imaginary part of the coherency function have been proposed. Of note, the imaginary part of the coherency function over frequency bands, the so-called imaginary coherence (ICOH), has been proposed as a FC index [15] that carries information about phase delay (i.e., phase synchronization) in oscillatory regimes between remote brain regions. However, due to the normalization of the coherence that involves the real part of the spectrum, non-interacting sources cause a decrease in ICOH. Consequently, although volume conduction cannot explain non-zero ICOH, it can still impact its value [10]. Moreover, the magnitude of ICOH depends on both the amplitude of the signals and the magnitude of the phase delay.

Further phase synchronization measures are based on the notion of instantaneous phase $\Phi_m(t)$ of a signal. Given a band-pass filtered MEG time series $Y_m(t)$, its Hilbert transform $\tilde{Y}_m(t)$ can be used to estimate $\Phi_m(t) \triangleq \arctan \frac{\tilde{Y}_m(t)}{Y_m(t)}$. As a robust indicator for phase syncronization between two signals m, m', the phase lag index (PLI) has been defined as

$$\mathrm{PLI}_{mm'}(k) \triangleq \left| \mathbb{E}\{\mathrm{sign}(\Phi_m(t_k) - \Phi_{m'}(t_k))\} \right|, \qquad (2)$$

where $t_k = k/f_s$ is a sampled time point and f_s the sampling frequency. Thus, PLI quantifies to which extent the phase of one signal leads (or lags) over the other [10]. By construction, $\mathrm{PLI} \in (0, 1)$, with large PLI indicating strong synchronization. PLI is not sensitive to phase synchronization with zero phase lag, the magnitude of phase delays or that of signals. Yet, the discontinuity at zero of the phase difference entering in (2) causes issues in the presence of noise. To overcome this issue, the weighted PLI (wPLI) [11] has been introduced,

$$\mathrm{wPLI}_{mm'}(f) \triangleq \frac{\left| \mathbb{E}\{|I_{mm'}(f)| \times \mathrm{sign}(I_{mm'}(f))\} \right|}{\mathbb{E}\{|I_{mm'}(f)|\}}, \qquad (3)$$

where $I_{mm'}(f) = \Im\{S_{mm'}(f)\}$ and $\Im$ stands for the imaginary part. wPLI uses the imaginary part of the cross-spectrum as a weight to reduce the contribution of small phase differences, which are easily perturbed by noise. It can be shown that wPLI has increased sensitivity to detecting (changes in) phase synchronization compared to PLI and ICOH [11].

B. Scale-free FC analysis in the complex wavelet domain

Inspired by above oscillatory regime FC indices, we now define multiscale FC indices for scale-free dynamics.

Complex wavelet transform. Let ψ denote a *mother wavelet*, i.e., an oscillating and sufficiently smooth reference pattern that is chosen such that the collection of dilated and translated templates $\{\psi_{j,k}(t) = 2^{-j/2}\psi(2^{-j}t - k)\}_{(j,k)\in\mathbb{Z}^2}$ of ψ form an orthonormal basis of $\mathcal{L}^2(\mathbb{R})$ [16]. The discrete wavelet transform (DWT) coefficients $d_Y(j,k)$ of a signal Y are defined as $d_Y(j,k) \triangleq \langle \psi_{j,k} | Y \rangle$ with $\langle \psi_{j,k} | Y \rangle = \int Y(t) 2^{-j} \psi_{j,k}(t) dt$ and are a mainstay in scale-free analysis, see, e.g., [2] and references therein.

As an alternative to the DWT, the complex wavelet transform (CoWT) can be defined. The key motivation for the use of CoWT in this work is that they allow to assess the *phase* of wavelet spectra. The design of an invertible, analytic wavelet transform is not straightforward, and in this contribution, we build on the solution proposed in [17], [18] named dual-tree complex wavelet transform (DT-CoWT). It consists of computing two DWTs using different wavelets $\psi^{(r)}$ and $\psi^{(\imath)}$ that are designed such that $\psi^{(r)} + \imath\psi^{(\imath)}$ is approximately analytic, i.e., $\psi^{(r)}(t) \approx \mathrm{Hilbert}\{\psi^{\imath}(t)\}$. The complex DT- CoWT

ISBN 978-90-827970-1-5 © EURASIP 2018

coefficients are defined as $d_Y(j,k) \triangleq d_Y^{(r)}(j,k) + \imath d_Y^{(i)}(j,k)$, with $d_Y^{(r)}(j,k) \triangleq \langle \psi_{j,k}^{(r)} | Y \rangle$ and $d_Y^{(i)}(j,k) \triangleq \langle \psi_{j,k}^{(i)} | Y \rangle$.

Scale-free phase synchronization measures. Given a pair of signals Y_m, $Y_{m'}$, the complex wavelet transform analogs to their Fourier spectra (for $m = m'$) and cross-spectrum (for $m \neq m'$) can be defined as

$$S_{mm'}^W(j) \triangleq \frac{1}{n_j} \sum_{k=1}^{n_j} d_{Y_m}(j,k) d_{Y_{m'}}^*(j,k) \tag{4}$$

where $n_j \approx \frac{N}{2^j}$ are the number of coefficients available at scale j, and * stands for the complex conjugate. Similarly, we define the wavelet coherence as

$$\text{w-COH}_{mm'}(j) \triangleq \frac{S_{mm'}^W(j)}{\sqrt{S_{mm}^W(j) S_{m'm'}^W(j)}}. \tag{5}$$

Note that unlike the standard DWT coherence used in, e.g., [9], $\text{w-COH}_{mm'}(j)$ is *complex-valued*. We denote the imaginary part as $\text{w-ICOH}_{mm'}(j) \triangleq \Im\{\text{w-COH}_{mm'}(j)\}$.

This allows us to define an alternative to the Fourier coherence based weighted phase lag index (3) that is suited to scale-free signals, the *wavelet weighted phase lag index* (w-wPLI)

$$\text{w-wPLI}_{mm'}(j) \triangleq \frac{\left| \sum_{k=1}^{n_j} \Im\{ d_{X_m}(j,k) d_{X_{m'}}^*(j,k) \} \right|}{\sum_{k=1}^{n_j} \left| \Im\{ d_{X_m}(j,k) d_{X_{m'}}^*(j,k) \} \right|}, \tag{6}$$

with the following key properties: i) it inherits from (3) the sensitivity to phase synchronizations and robustness to volume conduction effects and noise perturbations; ii) it can be relevantly assessed for infraslow scale-free dynamics thanks to the theoretical and practical benefits of the wavelet transform for self-similar signals [2]. For the numerical results reported here, we make use of q-shift wavelets as described in [18] and references therein (see, e.g., [19] for an alternative choice).

Illustration for synthetic data. The proposed multiscale phase synchronization indices are illustrated in Fig. 1 for one realization of operator fractional Brownian motion (ofBm), a multivariate version of self-similar fractional Brownian motion [20]. Results are obtained for two correlated ($\rho = 0.7$) ofBm components Y_1, Y_2 with different self-similarity exponents H (show in the top panel), without delay ($\Delta = 0$, second row) and with delay ($\Delta = 2$ samples, bottom row), respectively. They clearly indicate that while w-COH cannot distinguish volume conduction inducing instantaneous coupling ($\Delta = 0$) from non-trivial ($\Delta = 2$) phase synchronization, w-ICOH and w-wPLI provide unbiased estimators of phase synchronization that are at the same time robust to volume conduction and sensitive to phase coupling in scale-free signals.

III. Data

MEG recordings from 36 healthy participants (mean age: 22.1 +/- 2.2) were used in this study. All participants were right-handed, had normal hearing and normal or corrected-to-normal vision. Before the experiment, all participants provided a written informed consent in accordance with the Declaration of Helsinki (2008) and the local Ethics Committee on Human Research at NeuroSpin (Gif-sur-Yvette, France).

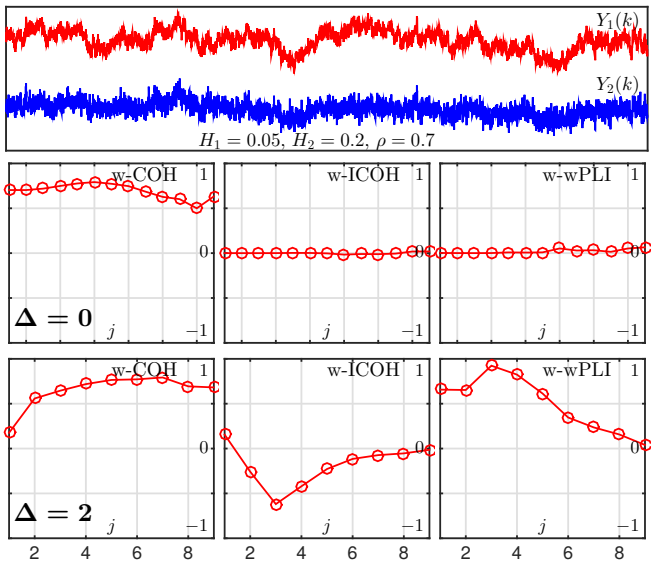

Fig. 1. **Scale-free phase synchronization indices.** Illustration for synthetic data: correlated components $Y_1(k)$ and $Y_2(k)$ of ofBm with different self-similarity exponents H (top panel) and complex wavelet transform multiscale indices w-COH (magnitude), w-ICOH and w-wPLI (from left to right) obtained for signals without delay (second row) and with delay of $\Delta = 2$ samples (i.e., for $Y_1(k)$, $Y_2(k+\Delta)$, bottom row).

The experiment consisted of interleaved blocks alternating between rest and task (detailed description in [12]). During the 5 minutes rest blocks, participants kept their eyes opened, and were not following any explicit instruction, allowing for the analysis of spontaneous fluctuations of MEG brain activity. The 12 minutes task blocks consisted of visual motion discrimination. Visual stimuli consisted of two colored and intermixed populations of moving dots. Participants were asked to tell which of the red or green cloud of dots was more coherent. Seven levels of visual coherence (15%, 25%, 35%, 45%, 55%, 75% and 95%) were tested; 28 trials per coherence level were collected for a total of 196 trials.

Brain activity was recorded in a magnetically shielded room using a 306 MEG system (Neuromag Elekta LTD, Helsinki). MEG signals originally sampled at 2 kHz were downsampled at 448 Hz. MEG signals were preprocessed to remove external and internal interferences, in accordance with accepted guidelines for MEG research [21]. Signal Space Separation (SSS) was applied with `MaxFilter` to remove exogenous artifacts and noisy sensors [22]. Ocular and cardiac artifacts were removed using Independent Component Analysis (ICA) on raw signals. ICA were fitted to raw MEG signals, and sources matching the ECG and EOG were automatically found and removed before signals reconstruction. Source localization from MEG signals was used to estimate cortical activity in 28 selected cortical regions of interest (ROIs) involved in task performance including frontal, somatosensory, temporal, parietal and occipital areas in [12].

IV. Scale-free FC analysis in MEG

A multi-scale FC analysis was performed on brain ongoing activity in order to explore the scale-free slow frequency

ISBN 978-90-827970-1-5 © EURASIP 2018

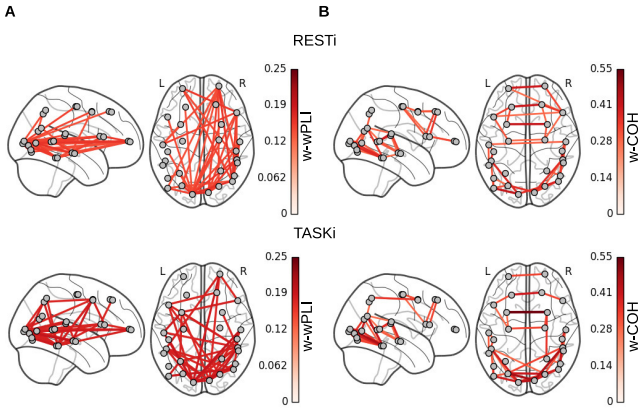

Fig. 2. **Top:** Strongest functional interactions estimated at rest using the complex wavelet wPLI (w-wPLI $\in (0,1)$, left) and coherence (w-COH $\in (0,1)$, right) indices, respectively. **Bottom:** Strongest functional interactions during task performance. Here colors code FC values between pairs of ROIs.

regime (0.1-1.5 Hz). The 28 ROI time series used for that purpose were thus not epoched as usually done for FC analysis in oscillatory regimes. Next, w-wPLI was computed to estimate bivariate phase coupling and compared to the complex wavelet coherence w-COH. For this, wavelet-based FC indexes were averaged over the scales corresponding to the frequency regime of interest. Two experimental conditions were considered, namely resting-state and task. The goal was to prove the gain brought by the w-wPLI approach in terms of sensitivity and specificity for detecting changes in FC patterns in the scale-free regime as compared to other FC measures.

FC networks in the scale-free regime. The group-level ($N = 36$) full 28×28 FC matrices extracted from rest and task-related activity and averaged in the scale-free regime ($8 \leqslant j \leqslant 12$ corresponding to $0.09\,\text{Hz} \leqslant f \leqslant 1.5\,\text{Hz}$) were filtered using a network density threshold [23]. The FC networks obtained using w-wPLI (Fig. 2A) and w-COH (Fig. 2B) present very different structures. In fact, coherence-based FC patterns show the predominance of short range interactions throughout the cortex both at rest and during task, likely resulting from residual common source effects which affect the real part of coherence [10]. In contrast, long range fronto-occipital connectivity emerges in w-wPLI based FC patterns. As a sanity check, we also assessed multi-scale FC using wavelet-based imaginary coherence w-ICOH. The latter measure yielded similar results as those obtained using w-wPLI. The w-wPLI index presumably represents a potential improvement over w-ICOH in detecting phase synchronization, as the former method is independent of the magnitude of the phase leads and lags, whereas the latter is strongly influenced by the phase of the wavelet coherence (5), cf. [10].

In order to investigate significant group-level differences in scale-free FC patterns between task and rest blocks, we performed a group-level paired t-test. The false discovery rate (FDR) control procedure was used to correct p-values for multiple comparisons. Interestingly, we observed a significant ($p < 0.01$) increase of w-wPLI in task as compared to rest (Fig. 3A). A similar FC pattern of differences was observed

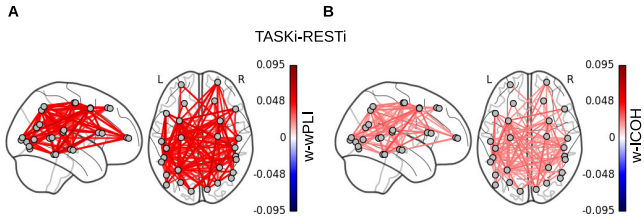

Fig. 3. **Left:** Statistically significant **Task vs Rest** FC pattern estimated using the w-wPLI index. **Right**: Same contrast using the wavelet based imaginary coherence (w-ICOH $\in (-1,1)$) index that also captures phase coupling. Here colors code the (**task-rest**) difference of FC values.

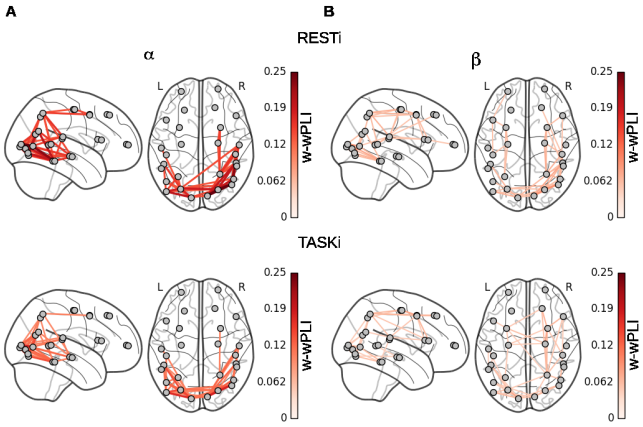

Fig. 4. **Top:** Strongest functional interactions estimated at rest using the w-wPLI index, in the α ($j = 5$, left) and β ($j = 4$, right) bands, respectively. **Bottom:** Strongest functional interactions estimated during task using the w-wPLI index, in the α (left) and β (right) bands, respectively.

using w-ICOH (Fig. 3B), while no significant difference was detected using w-COH. These results suggest a stronger efficiency of w-wPLI for detecting long range FC changes in the slow frequency regime as compared to w-ICOH.

FC networks in the oscillatory regime. In order to show the specificity of FC patterns in the scale-free regime, oscillatory regimes were then explored using w-wPLI and w-COH; for comparison purposes, the scales corresponding to the widely studied α (8-12 Hz) and β (13-30 Hz) rhythms were considered in this analysis. Specifically, at the scales corresponding to the α and β bands ($j = 5$ and $j = 4$, respectively) the density filtered networks based on the w-wPLI measure were characterized by short range FC, both at rest and during task blocks (Fig. 4), whereas long range connections dominate the pattern in the scale-free regime (Fig. 2A).

Moreover, α-band FC patterns (Fig. 4-left) showed higher phase synchronization values compared to the β-band (Fig. 4-right), and mainly involved occipital regions known to convey synchronized α oscillations. FC networks in the β-band showed different patterns involving frontal and parietal regions both at rest and during task. Interestingly, these estimated patterns support the commonly observed association of β oscillations, which are of relatively low amplitude, with endogenous and top-down controlled processing involving high level brain structures of frontal and parietal cortices. Here, the prevalence of short range connections in the observed β band FC reflects the sensitiveness of w-wPLI to shorter time delay at higher

ISBN 978-90-827970-1-5 © EURASIP 2018

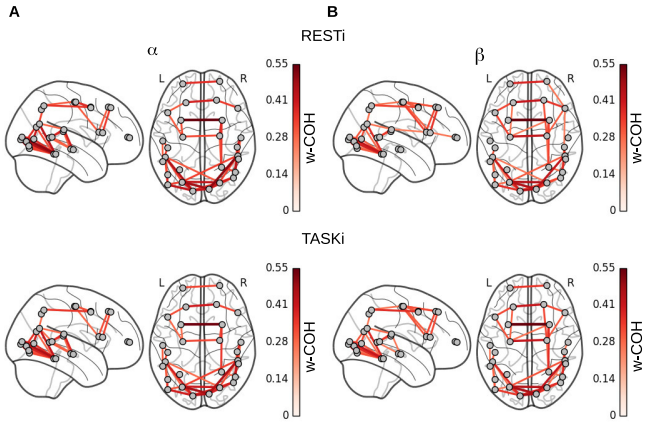

Fig. 5. **Top:** Strongest functional interactions estimated at rest using the w-COH phase coupling index, in the α ($j = 5$, left) and β ($j = 4$, right) bands, respectively. **Bottom:** Strongest functional interactions estimated during task using the w-COH index, in the α (left) and β (right) bands, respectively.

frequency regimes (Fig. 1). We performed the same analysis in the α and β-bands using the wavelet-based coherence (w-COH). The corresponding FC networks did not show the same centrality of connected occipital regions in α-range (Fig. 5A), neither the lower phase synchronization in β-range (Fig. 5B). On the other hand, these networks look very similar to the ones observed in the scale-free regime. This confirms the sensitivity of coherence-based FC indices to volume conduction effect regardless of the scale.

Interestingly, no significant difference was observed in the oscillatory regimes between rest and task-related networks using the tested multiscale measures. Overall, our results support the effectiveness of w-wPLI to detect changes of scale-free phase synchronization, and its robustness with respect to common source artifacts as compared to coherence measures.

V. Conclusion

This work proposed a novel multiscale phase synchronization measure for the assessment of functional connectivity in scale-free brain dynamics regime. To this end, the key intuitions of Fourier coherence based indices for oscillatory regimes, lending robustness against volume conduction effects in MEG, are combined with scale-free dynamics analysis in the complex wavelet transform domain. To the best of our knowledge, the proposed tool constitutes the only existing operational procedure for the robust quantification of phase synchronization in scale-free time series. Applied to MEG data for 36 individuals, this tool brought evidence for the presence of significant group-level scale-free FC networks, which are distinct from those classically uncovered with oscillatory regimes. It is noteworthy that only scale-free synchronization measures captured the variations in long-range phase synchronization between rest and task. Future work will focus on the functional role of those scale-free FC patterns.

Acknowledgment

Work supported by ANR-16-CE33-0020 MultiFracs, France.

References

[1] B. J. He, "Scale-free brain activity: past, present, and future," *Trends Cogn Sci*, vol. 18, no. 9, pp. 480–487, 2014.
[2] P. Abry, P. Flandrin, M. S. Taqqu, and D. Veitch, *Wavelets for the analysis, estimation, and synthesis of scaling data*. Wiley, 2000, pp. 39–88.
[3] D. Van de Ville, J. Britz, and C. M. Michel, "EEG microstate sequences in healthy humans at rest reveal scale-free dynamics," *Proc. Nat. Acad. Science*, vol. 107, no. 42, pp. 18 179–84, 2010.
[4] N. Dehghani, C. Bedard, S. S. Cash, E. Halgren, and A. Destexhe, "Comparative power spectral analysis of simultaneous elecroencephalographic and magnetoencephalographic recordings in humans suggests non-resistive extracellular media," *J. Comput. Neurosci.*, vol. 29, no. 3, pp. 405–421, 2010.
[5] N. Zilber, P. Ciuciu, P. Abry, and V. van Wassenhove, "Modulation of scale-free properties of brain activity in MEG," in *Proc. IEEE Int. Symp. Biomed. Imag. (ISBI)*, Barcelona, Spain, 2012, pp. 1531–1534.
[6] K. Gadhoumi, J. Gotman, and J. M. Lina, "Scale invariance properties of intracerebral EEG improve seizure prediction in mesial temporal lobe epilepsy," *PloS one*, vol. 10, no. 4, 2015.
[7] J. D. Power, A. L. Cohen, S. M. Nelson, G. S. Wig, K. A. Barnes, J. A. Church, A. C. Vogel, T. O. Laumann, F. M. Miezin, B. L. Schlaggar *et al.*, "Functional network organization of the human brain," *Neuron*, vol. 72, no. 4, pp. 665–678, 2011.
[8] P. Ciuciu, P. Abry, and B. J. He, "Interplay between functional connectivity and scale-free dynamics in intrinsic fMRI networks," *Neuroimage*, vol. 95, pp. 248–263, 2014.
[9] H. Wendt, G. Didier, S. Combrexelle, and P. Abry, "Multivariate Hadamard self-similarity: testing fractal connectivity," *Physica D*, vol. 356, pp. 1–36, 2017.
[10] C. J. Stam, G. Nolte, and A. Daffertshofer, "Phase lag index: assessment of functional connectivity from multi channel EEG and MEG with diminished bias from common sources," *Human brain mapping*, vol. 28, no. 11, pp. 1178–1193, 2007.
[11] M. Vinck, R. Oostenveld, M. Van Wingerden, F. Battaglia, and C. M. Pennartz, "An improved index of phase-synchronization for electrophysiological data in the presence of volume-conduction, noise and sample-size bias," *Neuroimage*, vol. 55, no. 4, pp. 1548–1565, 2011.
[12] N. Zilber, P. Ciuciu, A. Gramfort, and V. van Wassenhove, "Supramodal processing optimizes visual perceptual learning and plasticity," *Neuroimage*, vol. 93 Pt 1, pp. 32–46, 2014.
[13] A. K. Engel, P. Fries, and W. Singer, "Dynamic predictions: oscillations and synchrony in top–down processing," *Nature Reviews Neurosci.*, vol. 2, no. 10, p. 704, 2001.
[14] M. Siegel, T. H. Donner, and A. K. Engel, "Spectral fingerprints of large-scale neuronal interactions," *Nature Reviews Neurosci.*, vol. 13, no. 2, p. 121, 2012.
[15] G. Nolte, O. Bai, L. Wheaton, Z. Mari, S. Vorbach, and M. Hallett, "Identifying true brain interaction from EEG data using the imaginary part of coherency," *Clin Neurophysiol*, vol. 115, no. 10, pp. 2292–2307, 2004.
[16] S. Mallat, *A Wavelet Tour of Signal Processing*. San Diego, CA: Academic Press, 1998.
[17] N. Kingsbury, "Complex wavelets for shift invariant analysis and filtering of signals," *Appl. Comput. Harm. Anal.*, vol. 10, no. 3, pp. 234–253, 2001.
[18] I. W. Selesnick, R. G. Baraniuk, and N. C. Kingsbury, "The dual-tree complex wavelet transform," *IEEE Signal Process. Mag.*, vol. 22, no. 6, pp. 123–151, 2005.
[19] J.-M. Lina and M. Mayrand, "Complex daubechies wavelets," *Appl. Comput. Harm. Anal.*, vol. 2, no. 3, pp. 219–229, 1995.
[20] G. Didier and V. Pipiras, "Integral representations and properties of operator fractional Brownian motions," *Bernoulli*, vol. 17, no. 1, pp. 1–33, 2011.
[21] J. Gross, S. Baillet, G. R. Barnes, R. N. Henson, A. Hillebrand, O. Jensen, K. Jerbi, V. Litvak *et al.*, "Good practice for conducting and reporting MEG research," *Neuroimage*, vol. 65, pp. 349–363, 2013.
[22] S. Taulu and J. Simola, "Spatiotemporal signal space separation method for rejecting nearby interference in MEG measurements," *Physics in Medicine & Biology*, vol. 51, no. 7, p. 1759, 2006.
[23] F. De Vico Fallani, V. Latora, and M. Chavez, "A topological criterion for filtering information in complex brain networks," *PLoS computational biology*, vol. 13, no. 1, p. e1005305, 2017.